Comparison of the conformation of floral odorants: an NMR and molecular dynamics study †

Cecilia Anselmi,[a] Andrea Bernini,[b] Anna Buonocore,[a] Marisanna Centini,[a] Maria L. Paoli[a] and Alessandro Sega *[a]

[a] *Dipartimento Farmaco Chimico Tecnologico, Università di Siena, Via Aldo Moro 53100, Siena, Italy*
[b] *Dipartimento di Biologia Molecolare, Università di Siena, Siena, Italy*

Received (in Cambridge, UK) 30th May 2002, Accepted 10th July 2002
First published as an Advance Article on the web 30th July 2002

Odorous molecules, *cis*- and *trans*-4-methylcyclohexyl tetrahydrofuran-2-yl or pyranyl ethers, have been studied from the points of view of conformation and dynamics with the aim of extracting information on the relationships between white flower odour and structure. Both NMR and molecular dynamics analyses showed that *cis* derivatives, endowed with a main white flower note, have a bent structure corresponding to an oval molecular shape; the *trans* derivatives, exhibiting different odours, possess an extended structure corresponding to a cylindrical molecular shape. This comparison was also applied to two aromatic ethers both with a main floral note, 4-*tert*-butylphenyl tetrahydropyran-2-yl ether and 4-isopropylphenyl tetrahydrofuran-2-yl ether. These molecules also have similar conformations. All conformations for all molecules are independent of the solvent used, $CDCl_3$ or [$^2H_6$]DMSO (NMR) or vacuum, $CHCl_3$ or DMSO (molecular dynamics).

Introduction

The characteristic odour of the lily of the valley (muguet) has been the subject of great interest and research work for a long time.[1,2] The essential oil contains a great number of compounds, but none of them reproduces the typical note of muguet.[3] Despite the great interest in perfumery for this odour, natural lily of the valley oil is not commercially available; therefore, synthetic substitutes have been sought and employed with some success.

Although many compounds have been synthesised, the molecular parameters related to the odour of white flowers have not yet been clearly defined. Some results seem to indicate strict requirements in the stereochemistry of the odorants, within certain classes of compounds, such as hydroxy ketones and hydroxy aldehydes, derivatives of *p*-menthane and iridane, where *cis*/*trans* isomers or diastereoisomers differ dramatically in their odour potency.[4] However, the presence of two functional groups does not seem to be a requisite for the odour of muguet, which is well reproduced in compounds containing an aldehyde carbonyl as the sole functional group.

To provide more information on the relationships between chemical structure and the odour of white flower, epitomised by the note of muguet, we synthesised a series of tetrahydropyranyl and tetrahydrofuranyl ethers, bearing some similarity in molecular shape to the structures already known.[5,6] Among the compounds synthesised, we found molecules endowed with an intense white flower odour like *cis*-4-methylcyclohexyl tetrahydrofuran-2-yl ether (**1-*cis***) and *cis*-4-methylcyclohexyl tetrahydropyran-2-yl ether (**2-*cis***), whereas the structurally related *trans*-4-methylcyclohexyl tetrahydrofuran-2-yl ether (**1-*trans***) and *trans*-4-methylcyclohexyl tetrahydropyran-2-yl ether (**2-*trans***) do not possess this odour (*cis* and *trans* refer to relative orientations of H-6 and H-9 or H-7 and H-10 for **1** and **2** respectively; see Fig. 1). These molecules, differing in stereochemistry and in odour, were chosen for an NMR and molecular dynamics study with the aim of completely defining their molecular shape.

The results of this investigation could suggest strategies for designing new odorants with a white flower note. In order to achieve clearer insight into the relationships between molecular shape and white flower odour, we also chose for this study compounds **3**, 4-isopropylphenyl tetrahydrofuran-2-yl ether, and **4**, 4-(*tert*-butyl)phenyl tetrahydropyran-2-yl ether (see Fig. 1), where the cycloalkyl moiety was substituted by an aromatic ring (both molecules have an intense white flower odour).

The NMR study was performed in two solvents of different polarity, $CDCl_3$ and [$^2H_6$]DMSO, while the molecular dynamics analysis was done *in vacuo*, $CHCl_3$ and DMSO to mimic the different environments that the odorant molecules could meet on their way to the olfactory receptors.

Results and discussion

2.1 NMR: relaxation rate analysis

^1H and ^{13}C NMR assignments were made on the basis of decoupling and 2D (COSY and HETCOR; INADEQUATE for compounds **1** and **2**) NMR experiments. The numbering system for the compounds investigated is shown in Fig. 1.

The relative stereochemistry of compounds **2**–**4** was determined from the proton coupling constants ($J_{2,3ax}$) of the protons bonded to the bridgehead carbon atom(s). The presence of an axial–axial coupling constant (11–12 Hz) in **2** and **4** defines the geometry. Moreover, it has been demonstrated[7] that in 2-alkoxytetrahydropyranyl ethers the chemical shift (δ) of C-2 is also determined by the position of the alkoxy substituent: if this substituent is in an axial position the δ range of C-2 is 96.9–99.2 ppm, whereas if it is in an equatorial position the same range is 101.5–103.6 ppm. The conclusions that can be drawn from the ^{13}C NMR data (see Tables 1–4) indicate that the substituents on the tetrahydropyranyl rings are always in an axial position (anomeric effect[8]). According to the

† Electronic supplementary information (ESI) available: additional NMR data for compounds **1**–**4**. See http://www.rsc.org/suppdata/p2/b2/b205255e/

Table 1 Chemical shifts (δ) and spin–lattice relaxation rates,[a] R_1 ($1/T_1$), of the carbons of compounds **1-*trans*** and **1-*cis*** (0.1 mol dm^{-3} solutions in $CDCl_3$ and [$^2H_6$]DMSO, T = 298 K)

	Compound **1-*trans***				Compound **1-*cis***			
	$CDCl_3$		[$^2H_6$]DMSO		$CDCl_3$		[$^2H_6$]DMSO	
	δ (ppm)	R_1/s^{-1}	δ (ppm)	R_1/s^{-1}	δ (ppm)	R_1/s^{-1}	δ (ppm)	R_1/s^{-1}
C-2	101.8	0.19 ± 0.01	101.1	0.30 ± 0.02	101.9	0.16 ± 0.01	101.3	0.26 ± 0.02
C-6	75.2	0.18 ± 0.01	74.3	0.31 ± 0.02	71.4	0.16 ± 0.01	70.2	0.26 ± 0.02
C-5	66.5	0.30 ± 0.02	65.7	0.51 ± 0.02	66.5	0.26 ± 0.02	65.7	0.35 ± 0.02
C-7 or C-11	33.9	0.30 ± 0.02	33.5	0.52 ± 0.02	32.6	0.30 ± 0.02	32.2	0.54 ± 0.02
C-8 or C-10	33.5	0.32 ± 0.02	33.0	0.51 ± 0.02	31.1	0.30 ± 0.02	30.6	0.52 ± 0.02
C-10 or C-8	33.4	0.30 ± 0.02	32.9	0.52 ± 0.02	29.7	0.31 ± 0.02	29.0	0.54 ± 0.02
C-3	32.6	0.32 ± 0.02	31.6	0.53 ± 0.02	29.5	0.25 ± 0.02	29.2	0.33 ± 0.02
C-9	32.0	0.19 ± 0.01	31.5	0.31 ± 0.02	31.1	0.17 ± 0.01	30.7	0.27 ± 0.02
C-11 or C-7	32.0	0.31 ± 0.02	32.1	0.50 ± 0.02	28.9	0.32 ± 0.02	28.6	0.51 ± 0.02
C-4	23.6	0.29 ± 0.02	23.1	0.50 ± 0.02	23.7	0.26 ± 0.02	23.2	0.34 ± 0.02
C-12	22.0	0.34 ± 0.02	21.9	0.52 ± 0.02	21.5	0.27 ± 0.02	21.7	0.40 ± 0.02

[a] (±) Figures denote approximate 95% confidence limits of the exponential regression analysis.

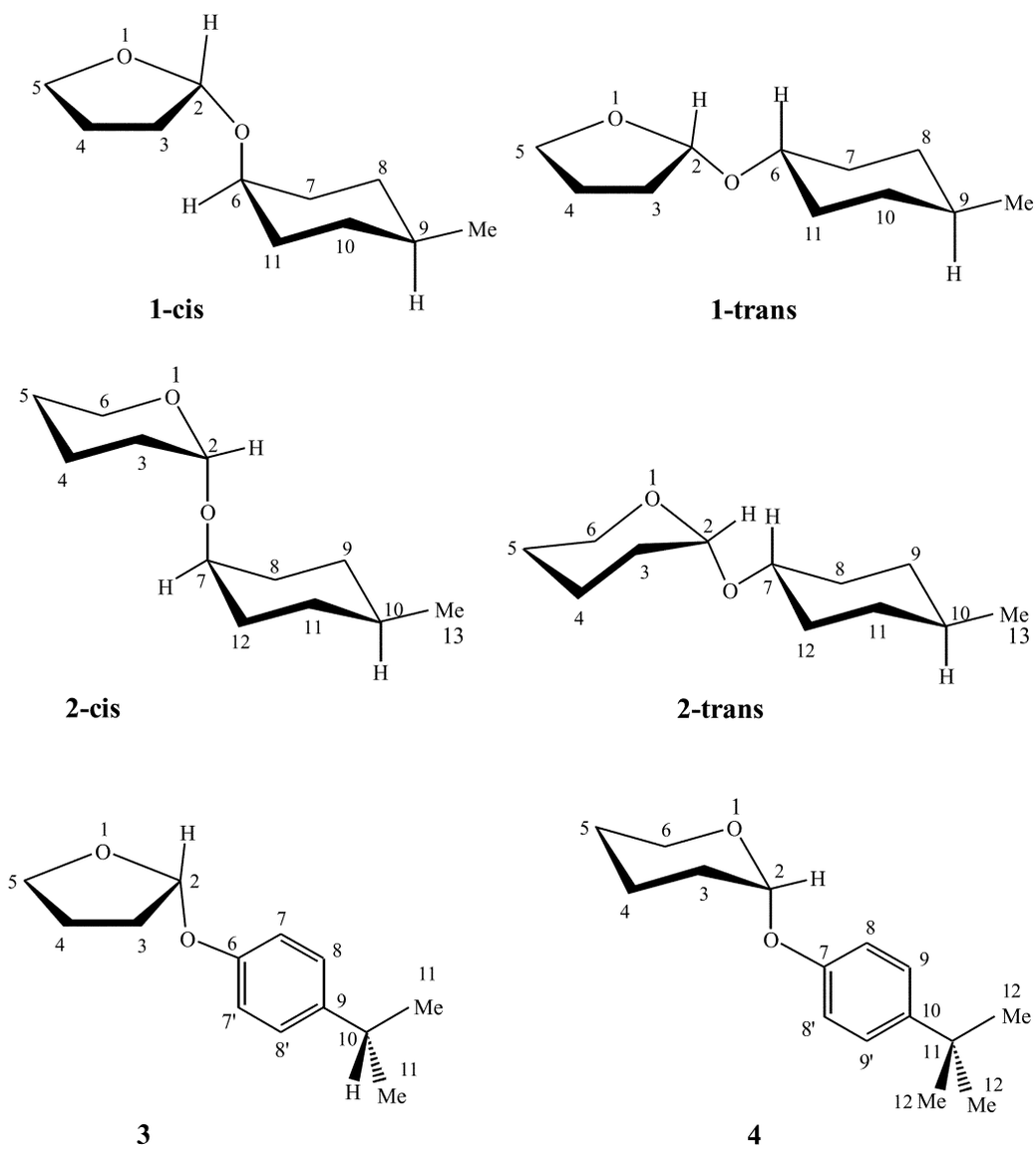

Fig. 1

above rationale, we can also infer from the chemical shifts of the C-2 carbon atoms in tetrahydrofuranyl rings (compounds **1** and **3**) that the substituents on this atom are in a pseudo-equatorial position (see Tables 1–3). Thus deductions from ^{13}C NMR chemical shifts are in complete agreement with those made from proton–proton coupling constants.

It is known that ^{13}C NMR relaxation rates ($R_1 = 1/T_1$) are almost exclusively determined by dipolar interactions with directly bonded or nearby protons, thus allowing suitable determination of the molecular dynamics.[9,10] Analysis of the R_1 values of the carbons in compound **1-*cis*** (Table 1) reveals that 1) the methine carbons, C-2, C-6 and C-9, have almost equal

Table 2 Chemical shifts (δ) and spin–lattice relaxation rates,[a] R_1 ($1/T_1$), of the carbons of compounds **2-*trans*** and **2-*cis*** (0.1 mol dm^{-3} in $CDCl_3$ and [$^2H_6$]DMSO, T = 298 K)

	Compound **2-*trans***				Compound **2-*cis***			
	$CDCl_3$		[$^2H_6$]DMSO		$CDCl_3$		[$^2H_6$]DMSO	
	δ (ppm)	R_1/s^{-1}	δ (ppm)	R_1/s^{-1}	δ (ppm)	R_1/s^{-1}	δ (ppm)	R_1/s^{-1}
C-2	96.7	0.22 ± 0.01	95.9	0.42 ± 0.02	96.7	0.18 ± 0.01	95.8	0.31 ± 0.02
C-7	75.1	0.21 ± 0.01	74.3	0.43 ± 0.02	71.0	0.19 ± 0.01	69.8	0.31 ± 0.02
C-6	62.7	0.46 ± 0.02	61.6	0.85 ± 0.03	62.7	0.36 ± 0.02	61.5	0.65 ± 0.03
C-10	32.0	0.21 ± 0.01	31.5	0.42 ± 0.02	31.4	0.19 ± 0.01	30.7	0.32 ± 0.02
C-3	31.3	0.45 ± 0.02	30.8	0.85 ± 0.03	31.2	0.35 ± 0.02	30.9	0.63 ± 0.03
C-8 or C-12	33.7	0.36 ± 0.02	33.3	0.70 ± 0.03	31.1	0.38 ± 0.02	30.5	0.61 ± 0.03
C-9 or C-11	33.7	0.36 ± 0.02	33.1	0.68 ± 0.03	29.7	0.35 ± 0.02	29.2	0.64 ± 0.03
C-11 or C-9	33.4	0.38 ± 0.02	32.8	0.68 ± 0.03	29.4	0.36 ± 0.02	28.9	0.62 ± 0.03
C-12 or C-8	31.8	0.36 ± 0.02	31.4	0.70 ± 0.03	28.6	0.35 ± 0.02	28.1	0.62 ± 0.03
C-5	25.6	0.43 ± 0.02	25.1	0.82 ± 0.03	25.6	0.39 ± 0.02	25.1	0.61 ± 0.03
C-13	22.0	0.41 ± 0.02	21.8	0.61 ± 0.03	21.6	0.32 ± 0.02	21.7	0.48 ± 0.02
C-4	20.0	0.44 ± 0.02	19.4	0.86 ± 0.03	20.0	0.37 ± 0.02	19.4	0.64 ± 0.03

[a] (±) Figures denote approximate 95% confidence limits of the exponential regression analysis.

Table 3 Chemical shifts (δ) and spin–lattice relaxation rates,[a] R_1 ($1/T_1$), of the protonated carbons of compound **3** (0.1 mol dm^{-3} in $CDCl_3$ and [$^2H_6$]DMSO, T = 298 K)

	$CDCl_3$		[$^2H_6$]DMSO	
3	δ (ppm)	R_1/s^{-1}	δ (ppm)	R_1/s^{-1}
C-6	155.2		154.8	
C-9	141.9		141.2	
C-7,7′	116.4	0.24 ± 0.01	116.3	0.54 ± 0.02
C-8,8′	127.2	0.24 ± 0.01	126.9	0.54 ± 0.02
C-2	102.4	0.21 ± 0.01	101.9	0.40 ± 0.02
C-5	67.9	0.26 ± 0.01	67.2	0.51 ± 0.02
C-10	33.3	0.15 ± 0.01	32.6	0.37 ± 0.02
C-3	32.7	0.31 ± 0.01	32.1	0.69 ± 0.03
C-11,11′	24.1	0.47 ± 0.02	24.0	0.83 ± 0.03
C-4	23.5	0.27 ± 0.01	23.0	0.58 ± 0.03

[a] (±) Figures denote approximate 95% confidence limits of the exponential regression analysis.

Table 4 Chemical shifts (δ) and spin–lattice relaxation rates,[a] R_1 ($1/T_1$), of the protonated carbons of compound **4** (0.1 mol dm^{-3} in $CDCl_3$ and [$^2H_6$]DMSO, T = 298 K)

	$CDCl_3$		[$^2H_6$]DMSO	
4	δ (ppm)	R_1/s^{-1}	δ (ppm)	R_1/s^{-1}
C-7	154.8		154.2	
C-10	144.3		143.6	
C-9,9′	126.1	0.27 ± 0.01	125.8	0.48 0.02
C-8,8′	115.9	0.27 ± 0.01	115.9	0.48 0.02
C-2	96.5	0.24 ± 0.01	95.8	0.42 0.02
C-6	62.0	0.52 ± 0.02	61.4	0.92 0.03
C-11	34.1		33.7	
3 × CH_3	31.5	0.56 ± 0.02	31.2	1.00 0.04
C-3	30.4	0.48 ± 0.02	29.8	0.92 0.03
C-5	25.3	0.67 ± 0.02	24.6	1.25 0.04
C-4	18.9	0.51 ± 0.02	18.6	0.86 0.03

[a] (±) Figures denote approximate 95% confidence limits of the exponential regression analysis.

relaxation rates; 2) the relaxation rates of the methylene carbons of the cyclohexyl moiety are close to one another and their values are double those of the methine carbons, while those of the tetrahydrofuranyl moiety are somewhat lower, but still close to one another; 3) motions are slower in [$^2H_6$]DMSO than in $CDCl_3$.

These experimental observations suggest that internal motions are very restricted, hence this molecule should have a well-defined main mean conformation in both solvents. The correlation time (τ_c) of the molecule can be evaluated from the relaxation rates of methine carbons considering that they are almost equal regardless of the relative orientations of the corresponding C–H vectors. As all protonated carbons exhibit maximum ^{13}C {^1H} nuclear Overhauser effects (NOEs), by applying eqn. (1), where r_{CH} is the length of the C–H bond and n is the number of protons attached to the carbon under consideration, it is possible to evaluate τ_c (see Table 5) in both solvents:

$$\frac{1}{nT_1} = \frac{\hbar^2 \gamma_H^2 \gamma_C^2}{r_{CH}^6} \tau_c \qquad (1)$$

Application of this analysis to compound **1-*trans*** reveals some features that we also found for its *cis* isomer, *i.e.* the relaxation rates of the methine carbons are almost equal and motions are slower in [$^2H_6$]DMSO than in $CDCl_3$. However, there is one important difference: the relaxation rates of the methylene carbons are close to one another not only within each ring but also among themselves, and they are not twice the values of the relaxation rates for C-2, C-6 and C-9 (see Table 1). This fact may well reflect a change in the main rotational axis with respect to **1-*cis***, and, hence, very probably a change in the main mean conformation. Internal motions are very restricted in both solvents. The main correlation time, τ_c (**1-*trans***), can be evaluated from eqn. (1) and its values in both solvents are reported in Table 5.

In compounds **2-*cis*** and **2-*trans*** the same analysis gives results close to those of **1-*cis*** and **1-*trans*** respectively (see Table 5). The main difference in the motional features in these compounds is thus determined by the relationship between the relaxation rates of the methylene carbons (R_{CH_2}) and those of the methine carbons (R_{CH}). In molecules **1-*cis*** and **2-*cis*** the ratio R_{CH_2}/R_{CH} is close or equal to 2, hence suggesting a more or less isotropic motion, whereas in **1-*trans*** and **2-*trans*** this conclusion does not hold true and there is probably a main rotational axis. On the basis of these facts a change in the main conformation is to be expected on passing from compounds **1-*cis*** and **2-*cis*** to compounds **1-*trans*** and **2-*trans***.

Inspection of the structures of these compounds reveals that the distance between the protons bonded to the bridgehead carbon atoms is the key parameter to be evaluated in order to gain knowledge of their main conformations. A measure of the distances H-2–H-6 ($r_{2,6}$), in **1-*cis*** and **1-*trans***, and H-2–H-7 ($r_{2,7}$), in **2-*cis*** and **2-*trans***, can be obtained through analysis of non-selective (R^i_{ns}), mono-selective (R^i_s), and double-selective

Table 5 Correlation times (τ_c/s) of compounds **1** and **2**

	$CDCl_3$			$[^2H_6]DMSO$		
	τ_c(THP)	τ_c(THF)	τ_c(Cy)	τ_c(THP)	τ_c(THF)	τ_c(Cy)
1-*trans*		0.82×10^{-11}	0.82×10^{-11}		0.14×10^{-10}	0.15×10^{-10}
1-*cis*		0.74×10^{-11}	0.79×10^{-11}		0.12×10^{-10}	0.13×10^{-10}
2-*trans*	1.07×10^{-11}		0.98×10^{-11}	0.19×10^{-10}		0.20×10^{-10}
2-*cis*	0.84×10^{-11}		0.93×10^{-11}	0.14×10^{-10}		0.15×10^{-10}

Table 6 Non-selective (R_{ns}), selective (R_s) and double-selective (R_{ds}) proton relaxation rates[a] (in s^{-1}) of selected protons of compounds **1**–**4** (0.1 mol dm^{-3} in $CDCl_3$ and $[^2H_6]DMSO$, T = 298 K)

		$CDCl_3$			$[^2H_6]DMSO$		
Compound	Proton	R_{ns}	R_s	R_{ds}	R_{ns}	R_s	R_{ds}
1-*trans*	H-2	0.33	0.26	$R^2_{2,6}$ 0.29	0.55	0.38	$R^2_{2,6}$ 0.50
	H-6	0.32	0.24	$R^6_{2,6}$ 0.27	0.61	0.43	$R^6_{2,6}$ 0.51
1-*cis*	H-2	0.26	0.22	$R^2_{2,6}$ 0.23	0.33	0.26	$R^2_{2,6}$ 0.28
	H-6	0.28	0.24	$R^6_{2,6}$ 0.25	0.39	0.32	$R^6_{2,6}$ 0.34
2-*trans*	H-2	0.41	0.33	$R^1_{2,7}$ 0.36	0.68	0.49	$R^1_{2,7}$ 0.53
	H-7	0.36	0.45	$R^6_{2,7}$ 0.48	0.68	0.48	$R^6_{2,7}$ 0.52
2-*cis*	H-2	0.38	0.29	$R^1_{2,7}$ 0.30	0.53	0.39	$R^1_{2,7}$ 0.41
	H-7	0.36	0.23	$R^6_{2,7}$ 0.24	0.75	0.54	$R^6_{2,7}$ 0.56
3	H-2	0.30	0.24	$R^2_{2,7}$ 0.27	0.48	0.35	$R^2_{2,7}$ 0.38
	H-7,7′	0.28	0.23	$R^7_{2,7}$ 0.26	0.45	0.37	$R^7_{2,7}$ 0.40
				$R^7_{7,8}$ 0.25			$R^7_{7,8}$ 0.41
	H-8,8′	0.31	0.26	$R^8_{7,8}$ 0.28	0.55	0.43	$R^8_{7,8}$ 0.47
4	H-2	0.39	0.32	$R^1_{2,8}$ 0.34	0.79	0.58	$R^1_{2,8}$ 0.62
	H-8,8′	0.33	0.26	$R^7_{2,8}$ 0.28	0.62	0.47	$R^7_{2,8}$ 0.51
				$R^7_{8,9}$ 0.31			$R^7_{8,9}$ 0.58
	H-9,9′	0.35	0.28	$R^8_{8,9}$ 0.33	0.64	0.47	$R^8_{8,9}$ 0.59

[a] Errors were evaluated within ±2.3 and ±2% (all experiments were performed three times).

Table 7 Proton–proton distances (Å) in compounds **1**–**4** estimated from relaxation rates (a) and $^1H\{^1H\}$ NOEs (b)

Compound	$CDCl_3$ (a)	$CDCl_3$ (b)	$[^2H_6]DMSO$ (a)	$[^2H_6]DMSO$ (b)
1-*trans*	$r_{2,6} = 2.1 \pm 0.1_5$		$r_{2,6} = 1.8 \pm 0.0_5$	
1-*cis*	—		$r_{2,6} = 2.4_5 \pm 0.2_5$	
2-*trans*	$r_{2,7} = 2.2 \pm 0.2$		$r_{2,7} = 2.3_5 \pm 0.2_5$	
2-*cis*	—		—	
3	$r_{2,7} = 2.3 \pm 0.1_5$	$r_{2,7} = 2.4$	$r_{2,7} = 2.6 \pm 0.2$	$r_{2,7} = 2.4$
4	$r_{2,8} = 2.90 \pm 0.2_5$	$r_{1,7} = 2.9$	$r_{2,8} = 3.0 \pm 0.3_5$	$r_{2,8} = 3.1$

(R_{ds}) proton spin–lattice relaxation rates. The use of proton relaxation rates as an aid to conformational studies in solution is a well-recognised method.[11–14] If the only contribution to the relaxation comes from the ^1H–^1H dipole–dipole relaxation mechanism, according to theory[13,14] and within the limits of the extreme narrowing region, eqn. (2) can be derived, where σ_{in} is the cross-relaxation rate for any proton pair,[15] r_{in} is the interproton distance and τ_c is the motional correlation time.

$$\sigma_{in} = \frac{1}{2}\frac{\hbar^2\gamma_H^4}{r_{in}^6}\tau_c \qquad (2)$$

The various values of σ_{in} can be estimated from the differences between corresponding biselective (R_{ds}) and selective (R^i_s) proton relaxation rate ($R_{ds} - R^i_s = \sigma_{in}$). Hence, proton–proton distances can be obtained from double-selective and mono-selective spin–lattice relaxation rates if τ_c is known from other sources.

The measured relaxation rates are reported in Table 6. However, not all the important distances can be evaluated once the experimental errors have been taken into consideration (see footnote in Table 6). The differences $R_{ds} - R^i_s$ of the relevant protons in compounds **1-*cis*** ($CDCl_3$) and **2-*cis*** (both solvents) do not allow a meaningful evaluation of the distances $r_{2,6}$ and $r_{2,7}$ respectively. The same distances can be evaluated for compounds **1-*trans*** and **2-*trans*** in both solvents and **1-*cis*** in $[^2H_6]DMSO$. These distances, $r_{2,6}$ and $r_{2,7}$, calculated using the appropriate correlation times (see Table 5) are reported in Table 7. Their values show that within each molecule these distances are independent of the nature of the solvent (*i.e.* $CDCl_3$ and $[^2H_6]DMSO$). The main mean conformations deriving from these distances are shown in Fig. 2 and are representative since the carbon R_1 analysis showed that internal motions are very restricted. Thus, on the basis of the conformations determined by stereochemistry and rotations around the C–O bonds of the oxygen bridge, compounds **1-*trans*** and **2-*trans*** can be said to have an extended structure corresponding to an overall cylindrical molecular shape, a picture that is consistent with the dynamics suggested for these molecules.

For compounds **1-*cis*** and **2-*cis*** the carbon relaxation rate analysis suggests a different overall molecular shape for these molecules. This observation cannot be supported by data related to distances $r_{2,6}$ and $r_{2,7}$. However, the only distance calculated for **1-*cis*** ($r_{2,6}$ in $[^2H_6]DMSO$) corresponds to main mean conformations with an oval shape, in agreement with the carbon relaxation rate analysis. Thus, evaluation of the molecular shape of the molecules of **1-*cis*** and **2-*cis*** requires a different approach (see later).

We have also studied compounds **3** and **4** (see Fig. 1), both having a white flower odour. Compounds **3** and **4** still maintain a certain resemblance to compounds **1** and **2**, respectively, but in both the cyclohexyl moiety has been substituted by aromatic units; in tetrahydrofuranyl ether **3**

Table 8 Correlation times (τ_c/s) of compounds **3** and **4**

	$CDCl_3$				$[^2H_6]DMSO$			
	τ_c(B)	τ_g(B)	τ_c(THP)	τ_c(THF)	τ_c(B)	τ_g(B)	τ_c(THP)	τ_c(THF)
3	0.15×10^{-10}	0.12×10^{-10}		0.83×10^{-11}	0.30×10^{-10}	0.10×10^{-10}		0.19×10^{-10}
4	0.38×10^{-10}	0.48×10^{-11}	0.11×10^{-10}		0.83×10^{-10}	0.82×10^{-11}	0.18×10^{-10}	

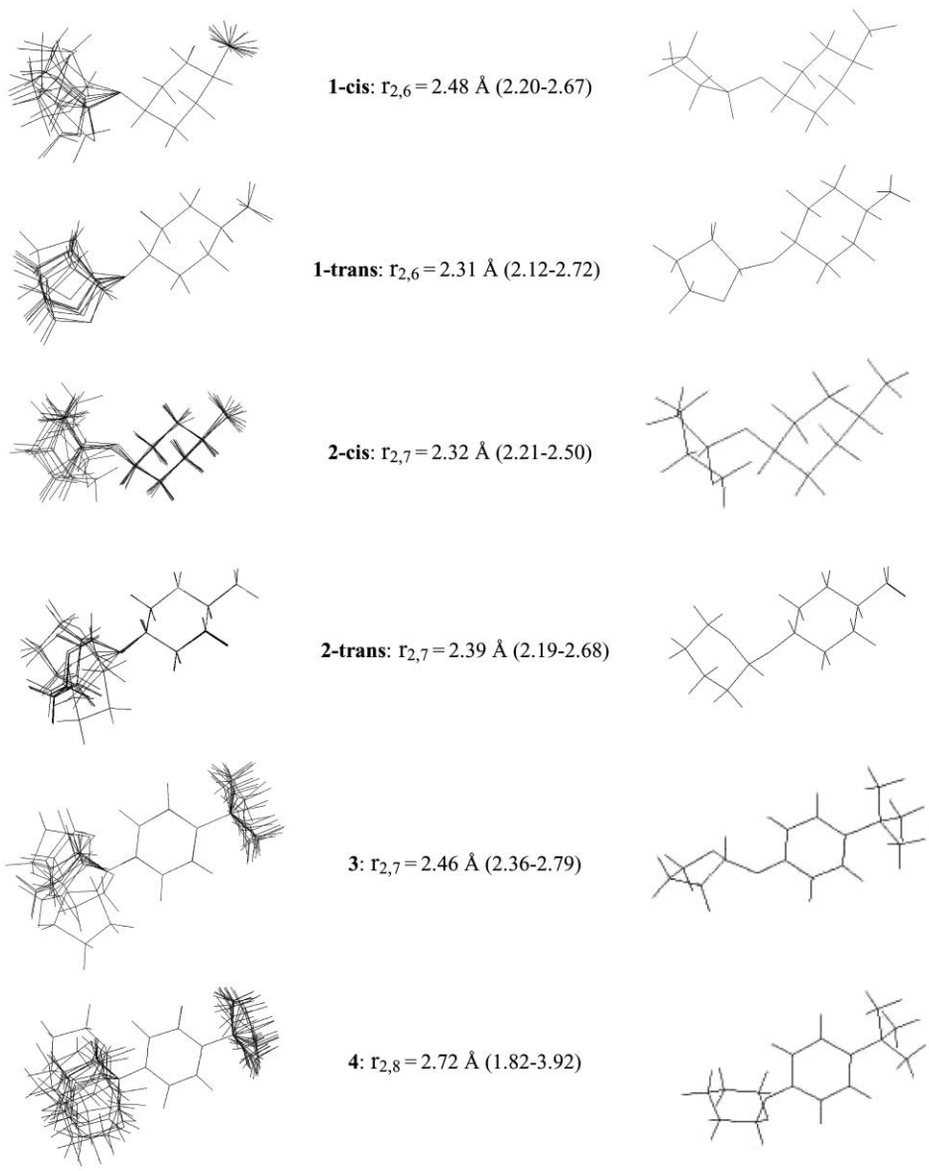

Fig. 2 Minimum energy conformation (right) and conformer bundle (left) within 3 kcal mol^{-1} from molecular dynamics in DMSO. Conformers were superposed using carbon atoms from the cyclohexane ring (compounds **1** and **2**) or aromatic ring (compounds **3** and **4**). The key distance for the minimum energy conformation of each compound is reported together with the upper and lower limits found in each bundle (in parentheses). The values of these distances show good agreement with those evaluated from the NMR analysis (see text).

there is a *p*-isopropylphenyl group and in the tetrahydropyranyl ether **4** there is a *p-tert*-butylphenyl group.

The relaxation rates ($R_1 = 1/T_1$) of protonated aromatic carbons are the same within each compound (see Tables 3 and 4), thus suggesting that C-6–C-9 and C-7–C-10 are the main rotational axes in **3** and **4**, respectively (as is to be expected for *p*-disubstituted benzenes). The dynamics of the aromatic rings can thus be described using an anisotropic model based on rotational reorientation around the main rotational axis with some degree of internal motion[16] [eqn. (3)] with $A = 0.25(3\cos^2\alpha - 1)^2$, $B = 3(\sin^2\alpha\cos^2\alpha)$ and $C = 0.75(\sin^4\alpha)$, where τ_c(B) is the main rotation correlation time, τ_g(B) the correlation time for vibrational motions of the aromatic ring, r_{CH} the length of the C–H bond, n the number of protons attached to the carbon under consideration and α the angle between the main rotation axis and the C–H vector. We could not evaluate the main correlation times of the aromatic moieties by applying eqn. (1) since none of the aromatic C–H vectors lies on or is parallel to the main rotational axes C-6–C-9 or C-7–C-10 [once known τ_c(B) allows the calculation of τ_g(B) from eqn. (3)].

$$\frac{1}{nT_1} = \frac{\hbar^2\gamma_H^2\gamma_C^2}{r_{CH}^6}\tau_c(B) \times \left[A + B\frac{6\tau_g(B)}{6\tau_g(B) + \tau_c(B)} + C\frac{3\tau_g(B)}{3\tau_g(B) + \tau_c(B)}\right] \quad (3)$$

This problem can, however, be overcome by using proton relaxation rates; in fact, in compound **3** the H-7–H-8 vector is

parallel to the main axis C-6–C-9 and by using double-selective and selective relaxation rates we can write eqn. (4):

$$R_{7,8}^7 - R_S^7 = \sigma_{7,8} = \frac{1}{2}\frac{\hbar^2\gamma_H^4}{r_{7,8}^6}\tau_c(B) \quad (4)$$

where $r_{7,8}$ is the H-7–H-8 interproton distance. This distance was determined from neutron scattering data, r = 2.45 Å. Hence, by introducing into eqn. (4) the appropriate values of the proton relaxation rates (see Table 5) it was possible to calculate the $\tau_c(B)$ value and, consequently, to know the $\tau_g(B)$ value from eqn. (3). A similar analysis holds for compound **4**. All the $\tau_c(B)$ and $\tau_g(B)$ values are reported in Table 8. In compound **3** internal motions within the aromatic ring are restricted in both solvents but especially in $CDCl_3$ where $\tau_c(B)$ and $\tau_g(B)$ have very close values (0.15×10^{-10} and 0.12×10^{-10} s respectively). In compound **4** there is a certain degree of internal motion for the aromatic ring in both solvents.

In $CDCl_3$ the relaxation rates of the methylene carbons (see Table 8) of the tetrahydrofuranyl moiety of compound **3** are very close to each other but their values are less than twice the value of the methine ring carbon (R_1 = 0.31–0.28 s^{-1} for C-3, C-4 and C-5 and R_1 = 0.21 s^{-1} for C-2), thus suggesting the presence of a preferential rotational axis. It is interesting to note that the other methine carbon, C-10, belonging to the isopropyl group has a relaxation rate which is close to that of C-2 [R_1(C-10) = 0.19]. These observations suggest a dynamic situation with restricted internal motions and in fact the main correlation time of the THF moiety [τ_c(THF)], calculated from eqn. (1) using the C-2 relaxation rate, does not differ greatly from the correlation time of the benzene ring [$\tau_c(THF) = 0.83 \times 10^{-11}$, $\tau_c(B) = 0.15 \times 10^{-10}$, $\tau_g(B) = 0.12 \times 10^{-10}$s; see Table 8). In [$^2H_6$]DMSO the only important difference is that motions are slower than in $CDCl_3$, whereas all other observations are in line with the former analysis in $CDCl_3$ [τ_c(THF) evaluated from eqn. (1) and using the relaxation rate of C-2 is 0.19×10^{-10} s while $\tau_c(B) = 0.30 \times 10^{-10}$ and $\tau_g(B) = 0.10 \times 10^{-10}$ s; see Table 8].

The relaxation rates of the methylene carbons within the tetrahydropyranyl (THP) ring of compound **4** have values that are not only close to each other, but are also double that of the methine carbon C-2, and this holds good for both solvents as shown in Table 4. The correlation time of this moiety [τ_c(THP)] was calculated from eqn. (1) using the R_1 value of C-2 and its value in both solvents is reported in Table 7. As can be seen, this value is midway between the corresponding $\tau_c(B)$ and $\tau_g(B)$ values rendering an overall dynamic picture of restricted internal motions.

The motional features of compounds **3** and **4** are thus consistent with the presence of a well-defined main mean conformation, as for compounds **1**–**2**. The relevant interproton distances that can give access to these conformations are those between H-2 and H-7, $r_{2,7}$, and between H-2 and H-8, $r_{2,8}$, for molecules **3** and **4**, respectively.

These distances can be evaluated from an analysis of the proton relaxation rates as already applied for compounds **1** and **2**. Indeed, eqns. (5) and (6),

$$R_{2,7}^2 - R_S^2 = \sigma_{2,7} = \frac{1}{2}\frac{\hbar^2\gamma_H^4}{r_{2,7}^6}\tau_c(B) \quad (5)$$

$$R_{2,8}^1 - R_S^1 = \sigma_{2,8} = \frac{1}{2}\frac{\hbar^2\gamma_H^4}{r_{2,8}^6}\tau_c(B) \quad (6)$$

where the correlation times are those of the corresponding benzene rings (the slowest correlation times for **3** and **4**, respectively), allow calculation of $r_{2,7}$ and $r_{2,8}$. Their values in both solvents are shown in Table 6 and are almost independent of the solvent nature for both molecules.

2.2 NMR: NOE analysis

It is also possible to calculate these distances from a nuclear Overhauser effect (NOE) analysis.[17] The relevant NOEs are reported in Table 9 for 0.1 M solutions in both solvents (the NOEs were also estimated in 0.01 M solutions and their values did not show any significant change). These NOEs allow evaluation of $r_{2,7}$ and $r_{2,8}$ since, by assuming the cross-saturation terms to be negligible, we can write eqns. (7) and (8):

$$\frac{f_{H\text{-}7}\ (H\text{-}8)}{f_{H\text{-}7}\ (H\text{-}2)} = \frac{r_{H\text{-}2,H\text{-}7}^6}{r_{H\text{-}7,H\text{-}8}^6} \quad (7)$$

$$\frac{f_{H\text{-}8}\ (H\text{-}9)}{f_{H\text{-}8}\ (H\text{-}2)} = \frac{r_{H\text{-}2,H\text{-}8}^6}{r_{H\text{-}8,H\text{-}9}^6} \quad (8)$$

The distances thus calculated are shown in Table 7 and they are in good to very good agreement with the corresponding distances evaluated from the proton relaxation rates.

This quantitative NOE study could not be carried out for compounds **1** and **2** since it was impossible to have access to the relevant parameters required for the application of equations like (7) or (8).

The main mean conformations of molecules **3** and **4** are shown in Fig. 2. Their molecular shapes are similar.

This NMR analysis allows the evaluation of important features of these molecules. However, the main mean conformations of compounds **1**-***trans***, **2**-***trans***, **1**-***cis*** (in [$^2H_6$]DMSO) **3** and **4** are based on dynamical parameters and one key distance, whereas for compounds **1**-***cis*** ($CDCl_3$) and **2**-***cis*** even these key distances are lacking.

2.3 Molecular dynamics analysis

In order to acquire deeper knowledge of the conformations of these molecules and the possibility of comparing their molecular shapes, we decided to support the NMR study with a molecular dynamics analysis. This analysis was done on all the compounds without introducing restraints based on the NMR results. As for the NMR study the dynamics was simulated in several environments: vacuum, $CHCl_3$ and DMSO. The molecular dynamics protocol reported in the Experimental section was applied to all molecules and environments.

The final 75 ps molecular dynamics trajectory was analysed in the search for conformers within 3 kcal mol^{-1} from the minimum energy value, and the relative structures were superimposed to show the molecular flexibility around the energy minimum more clearly. All the compounds showed very similar behaviour in the three environments, so only superimpositions in DMSO are reported. For molecules **1**-***trans*** and **2**-***trans*** it is shown that the conformers are close to those derived from NMR observations, while compounds **3** and **4** span a larger conformational space. For compounds **1**-***cis*** and **2**-***cis*** the conformers suggest an oval shape that fits the corresponding carbon relaxation rate analyses. The key distances, $r_{2,7}$ (**2**-***trans*** and **2**-***cis***), $r_{2,6}$ (**1**-***trans*** and **1**-***cis***), $r_{2,7}$ (**3**) and $r_{2,8}$ (**4**) evaluated for conformational minima and the range of values for these distances in the conformational bundle together with their corresponding conformers are reported in Fig. 2. The values of these distances can be compared with those determined from the NMR analysis (see Table 7). The two series of values are in good agreement.

2.4 Conformational space analysis

To further support the evaluation of the molecular shape an extensive conformational energy search was carried out on each

Table 9 Selected NOEs in compounds **3** and **4** (0.1 mol dm^{-3} in $CDCl_3$ and [$^2H_6$]DMSO, T = 298 K)

		$CDCl_3$		[$^2H_6$]DMSO	
Compound	Irradiated	Observed	NOE (%)	Observed	NOE (%)
3	H-8,8′	H-7,7′	10.3	H-7,7′	16.3
		H-10	3.9	H-2	−2.0
		H-11,11′	5.2	H-10	5.9
	H-7,7′	H-8,8′	10.3	H-8,8′	18.8
		H-2	5.2	H-2	7.7
	H-2	H-7,7′	10.7	H-8,8′	−3.9
				H-7,7′	17.4
	H-10	H-8,8′	5.0	H-8,8′	8.5
				H-7,7′	−3.4
4	H-9,9′	H-8,8′	17.3	H-8,8′	26.4
				H-2	−1.1
	H-8,8′	H-9,9′	11.2	H-9,9′	23.6
		H-2	4.6	H-2	5.0
	H-2	H-8,8′	6.3	H-8,8′	6.9
		H-9,9′	−1.8		

compound by rotating stepwise both dihedral angles connecting rings according to the protocol reported in the Experimental section. The dihedrals of interest were C3–C2–O–C6 and C2–O–C6–C7 for **1-*cis***, **1-*trans*** and **3**, C3–C2–O–C7 and C2–O–C7–C8 for **2-*cis***, **2-*trans*** and **4**. An isoenergetic contour plot chart of the conformational analysis is shown in Fig. 3 for compound **1-*cis*** in DMSO as an example.

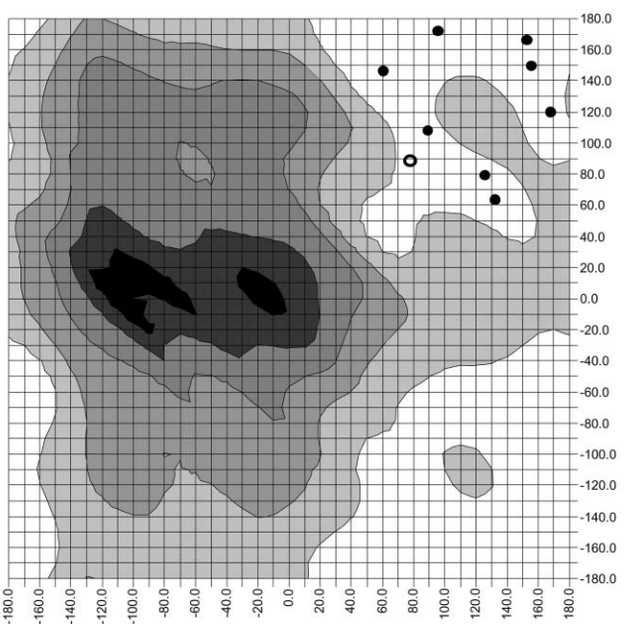

Fig. 3 Isoenergetic contour plot from the conformational search for compound **1-*cis***. The dihedral angles C3–C2–O–C6 and C2–O–C6–C7 are reported on the x and y axis, respectively. Isoenergetic contours are drawn in steps of 5 kcal mol^{-1} (larger than the range used for clustering molecular dynamics results to achieve clearer representation) and define greyscale areas from low (white) to high (black) energy. Filled and open circles represents respectively dihedral values for conformation bundle and minimum energy structures derived by molecular dynamics and reported in Fig. 2. All the conformations lie in the lowest energy area, showing good agreement between the two methods.

Analysis of the results reveals that the protons H-2 and H-6 in compounds **1-*cis*** and **1-*trans*** and protons H-2 and H-7 in compounds **2-*cis*** and **2-*trans*** face each other for conformations lying in the low energy area within 5 kcal mol^{-1} of the absolute minimum. It should be noted that such an area is rather large, so a small "twist" around the dihedrals is allowed and a conformational equilibrium can be hypothesised.

Similar behaviour can be predicted for compound **3**, with H-2 oriented toward H-7 (or H-7′), while an unfavourable energy is obtained when an oxygen atom from the tetrahydrofuran ring faces H-7. The energy barriers are rather lower than for the other compounds, so a larger equilibrium could be predicted than for **1** and **2**. For compound **4** the same observations are made as for **3**.

Thus, in closely correlated structures the stereochemistry and main mean conformation can be important in determining the odour. Indeed, the facts emerging from both the NMR and molecular dynamics studies suggest the following: i) compounds **1-*cis*** and **2-*cis*** have a very similar oval molecular shape that is clearly different from that of **1-*trans*** and **2-*trans*** (cylindrical shape); correspondingly **3** and **4** have similar molecular shapes; ii) conformation and also molecular shapes are independent of solvent or environment.

The reported study underlines, indeed, the importance of the molecular shape as one of the key parameters in determining the odour of molecules.[18,19]

Experimental

3.1 Nuclear magnetic resonance

The compounds under investigation were synthesised as previously described.[5,6] Solutions were made in 99.85% [$^2H_6$]DMSO (Merck) and $CDCl_3$ (Merck) and were carefully deoxygenated. NMR measurements were carried out with a Bruker AC-200 Fourier transform spectrometer. Chemical shifts were referred to internal TMS. Spin–lattice relaxation rates were measured using the inversion–recovery pulse sequence, 32 and 196 FIDs were collected for ^1H and ^{13}C T_1 measurements, respectively. Selective and double-selective relaxation rates were measured using inversion–recovery pulse sequences where the π pulse was given by the proton decoupler at selected frequencies at low power for relatively long times[15] (the typical experimental setting for a 180° pulse was 20–30 ms with 12–18 db attenuation). The selective rate was measured[20] in the initial slope approximation by considering only the first part of the recovery curve; $^1H\{^1H\}$ NOEs were measured with gated decoupling techniques using NOE difference pulse sequences. ^1H Homonuclear (COSY) (spectral width 2000 Hz, 1024 data points, 128 increments of 32 scans each, 4 dummy scans), ^{13}C–^1H heteronuclear (HETCOR) (^1H spectral width 2000 Hz, ^{13}C spectral width 4500 Hz, 4096 data points, 256 increments of 128 scans each, 4 dummy scans) and 2D-INADEQUATE (spectral width 4500 Hz, 2048 data points, 256 increments of 128 scans each, 4 dummy scans) experiments were performed according to standard sequences.[21–24]

3.2 Molecular dynamics

The conformational study was carried out *in vacuo*, $CHCl_3$ and DMSO using the AMBER force field and the AMBER soft-

ware.[25] The structures of the compounds were built from scratch, then a constant temperature dynamics with periodic temperature jumps[26] was employed: 8 ps MD at 300 K, temperature jumps at 600 K for 4 ps to provide enough energy to pass conformational barriers, four repetitions of this cycle. A 75 ps MD run at 300 K followed.

3.3 Conformational space evaluation

Molecular structures were built with standard angle and bond values, while previously described dihedrals were initially set to 0° and a force constraint of 40 kcal mol^{-1} deg^{-1} was applied; minimisation in the AMBER force field[25] followed until an energy gradient of 0.01 kcal mol^{-1} was reached and the total energy of the system recorded. In the subsequent steps the same procedure was repeated from scratch, the structure was built again with standard values and same constraints but by incrementing one dihedral by 10° each step while keeping the other fixed, until a complete rotation was performed for the former. At this point the latter dihedral was incremented by 10° and another complete rotation in 10° steps experienced by the other and so on. This gave a 36 × 36 matrix representing energies for each pair of dihedral angles values ranging from −180° to +180° in 10° steps.

References

1 P. Jellinek, *Prakticum des modernen Perfumeurs*, Huthig Verlag, Heidelberg, 1960.
2 M. J. Cook, *Drug Cosmet. Ind.*, 1970, **107**, 65.
3 M. Boelens, M. J. Wobben and J. Heydel, *Perfum. Flavor.*, 1980, **5**, 2.
4 G. Olhoff and W. Giersch, *Helv. Chim. Acta*, 1980, **63**, 76.
5 C. Anselmi, M. Centini, M. Mariani, A. Sega and P. Pelosi, *J. Agric. Food Chem.*, 1992, **40**, 853.
6 C. Anselmi, M. Centini, M. Mariani, A. Sega and P. Pelosi, *J. Agric. Food Chem.*, 1993, **41**, 781.
7 R. D. McKelvey, Y. Kawada, T. Sugawara and H. Iwamura, *J. Org. Chem.*, 1981, **46**, 4948.
8 *The Anomeric Effect and Associated Stereoelectronic Effects*, ed. G. R. J. Thatcher, ACS Symposium Series, American Chemical Society, Washington, DC, 1993.
9 F. W. Wehrli, in *Topics in carbon-13 NMR spectroscopy*, ed. G. C. Levy, Wiley, New York, 1976, vol. 2, p. 343.
10 J. R. Lyerla, Jr. and G. C. Levy, in *Topics in carbon-13 NMR spectroscopy*, ed. G. C. Levy, Wiley, New York, 1974, vol. 1, p. 74.
11 C. W. M. Grant, L. D. Hall and C. M. Preston, *J. Am. Chem. Soc.*, 1973, **95**, 7742.
12 L. D. Hall, *Chem. Soc. Rev.*, 1975, **4**, 401.
13 E. Gaggelli and G. Valensin, *Concepts Magn. Reson.*, 1992, **4**, 339.
14 E. Gaggelli and G. Valensin, *Concepts Magn. Reson.*, 1993, **5**, 19.
15 G. Valensin, G. Sabatini and E. Tiezzi, in *Advanced magnetic resonance techniques in systems of high molecular complexity*, ed. N. Niccolai and G. Valensin, Birkauser, Boston, 1986, p. 69.
16 A. Allerhand, D. Doddrell and R. Komoroski, *J. Chem. Phys.*, 1971, **55**, 189.
17 J. H. Noggle and R. E. Schirmer, *The Nuclear Overhauser Effect*, Academic Press, New York, 1971.
18 K. J. Rossiter, *Chem. Rev.*, 1996, **96**, 3201.
19 G. Fráter, J. A. Bajgrowicz and P. Kraft, *Tetrahedron*, 1998, **54**, 7633.
20 R. Freeman, H. D. Hill, B. L. Tomluison and L. D. Hall, *J. Chem. Phys.*, 1974, **61**, 4466.
21 W. P. Ane, E. Barthosdi and R. R. Ernst, *J. Chem. Phys.*, 1976, **64**, 2229.
22 J. A. Wilde and P. H. Bolton, *J. Magn. Reson.*, 1984, **59**, 343.
23 T. H. Mareci and R. Freeman, *J. Magn. Reson.*, 1982, **48**, 158.
24 D. L. Turner, *J. Magn. Reson.*, 1982, **49**, 175.
25 D. A. Pearlman, D. A. Case, J. W. Caldwell, W. S. Ross, T. E. Cheatham III, D. M. Ferguson, G. L. Seibel, U. C. Singh, P. K. Weiner and P. A. Kollman, AMBER 4.1, University of California, San Francisco, 1995.
26 J. Gharbi-Benarous, P. Ladam, M. Delaforge and J. Girault, *J. Chem. Soc., Perkin Trans. 2*, 1993, 2303.